Redox Processes of Cytochrome *c* Immobilized on Solid Supported Polyelectrolyte Multilayers

Inez M. Weidinger,[†] Daniel H. Murgida,[†] Wen-fei Dong,[‡] Helmuth Möhwald,[‡] and Peter Hildebrandt*[,†]

Institut für Chemie, Technische Universität Berlin, Sekr. PC14, Strasse des 17, Juni, D-10623 Berlin, Germany, and the Max-Planck-Institut für Kolloid- und Grenzflächenforschung, Am Mühlenberg 2, D-14424 Golm, Germany

Received: October 21, 2005

The heme protein cytochrome *c* (Cyt-c), immobilized on polyelectrolyte multilayers on a silver electrode, was studied by stationary and time-resolved surface-enhanced resonance Raman (SERR) spectroscopy to probe the redox site structure and the mechanism and dynamics of the potential-dependent interfacial processes. The layers were built up by sequential adsorption of polycations (poly[ethylene imine] (PEI); polyallylamine hydrochloride (PAH)) and polyanions (poly[styrene sulfonate] (PSS)). All multilayers terminated by PSS electrostatically bind Cyt-c. On PEI/PSS coatings, Cyt-c is peripherally bound and fully redox-active. Due to the interfacial potential drop, the apparent redox potential is lowered by 40 mV compared to that in solution. The rate constant for the heterogeneous electron transfer (ET) of ca. 0.1 s^{-1} is consistent with electron tunneling through largely ordered PEI/PSS layers. ET is coupled to a reversible conformational transition of Cyt-c that involves a change of the coordination pattern of the heme. Additional (PAH/PSS) double layers cause a broadening of the redox transition and a drastic negative shift of the redox potential, which is attributed to the formation of PSS/Cyt-c complexes. It is concluded that Cyt-c can effectively compete with PAH for binding of PSS, resulting in a rearrangement of the layered structure and a penetration of the PSS-bound Cyt-c into the PAH/PSS double layers. This conclusion is consistent with SERR intensity and quartz microbalance measurements. ET was found to be overpotential-independent and faster than that for PEI/PSS coatings, which is interpreted in terms of specific PSS/Cyt-c complexes serving as gates for the heterogeneous ET.

Introduction

Immobilization of redox-active proteins on electrodes is a central issue in bioelectronics.[1] Potential applications as biocatalysts or biosensors require an efficient and durable electronic communication between the biomolecule and the conducting solid support. Since direct adsorption of proteins on metal electrodes is generally associated with a slow and irreversible redox behavior as a result of protein structural changes,[2−4] electrodes have to be functionalized by biocompatible coatings such that the structure of the immobilized proteins remains largely preserved. Widely studied coatings are self-assembled monolayers (SAM) of bifunctional thiols or Langmuir−Blodgett (LB) films.[5−7] These systems are well-ordered and thus advantageous for investigating fundamental issues of protein immobilization, but they are not appropriate for biotechnological applications due to the time-consuming fabrication and their limited long-term stability.

Polyelectrolyte (PE) multilayers represent a promising alternative since they are cheap and easy to prepare such that upscaling is simple and economic. PE coatings are chemically and physically stable, and they exhibit large ion-exchange capacity, strong affinity for binding to metallic surfaces, water insolubility, prolonged retention of counterions, and rapid charge propagation rates. With the development of the layer-by-layer technique,[8] multicomponent polyelectrolyte multilayers can be created on electrode surfaces via iterative deposition of oppositely charged polyelectrolytes and thus allow a fine-tuning of the chemical and physical properties of the coatings. PE multilayer systems allow immobilization of relatively large quantities of proteins as demonstrated by UV−vis and IR absorption spectroscopy,[9−11] scanning angle reflectometry,[12] light scattering,[13] and quartz crystal microbalance measurements (QCM).[14,15] Up to now, however, the consequences of protein adsorption on PE-coated electrodes for the structural and functional properties are not yet understood in detail.

The redox protein cytochrome c (Cyt-c) has been shown to bind to PE-coated electrodes.[14] This small (12.5 kDa) soluble heme protein is one of the best characterized proteins[16] and, specifically, its behavior upon immobilization to solid supports, membranes, SAMs, or LB films has been extensively investigated by a variety of physicochemical techniques.[17] Thus, Cyt-c represents an ideal candidate to analyze, in detail, the consequences of immobilization on PE-coated electrodes for the molecular structure and functioning of an electron-transferring protein.

This issue is addressed in the present work using a silver electrode as a solid support for the PE deposition. Thus, it is possible to employ surface-enhanced resonance Raman spectroscopy (SERR) that selectively probes the redox site of the immobilized protein, i.e., a heme group, such that possible

* To whom correspondence should be addressed. Phone: +49-30-314-21419. Fax: +49-30-314-21122. E-mail: hildebrandt@chem.tu-berlin.de.
[†] Technische Universität Berlin.
[‡] Max-Planck-Institut Golm.

10.1021/jp056040c CCC: $33.50
Published on Web 12/08/2005

adsorption-induced structural changes in the heme pocket can be monitored.[18−22] Furthermore, potential-dependent and time-resolved SERR spectroscopy allows determination of the redox potentials and the electron transfer (ET) dynamics, thus giving insight into the molecular mechanism of the interfacial redox process.[20,23−26] Following previous reports that demonstrated preservation of redox activity of Cyt-c on poly(styrene sulfonate) (PSS) layers,[27,28] we were specifically interested in exploring how different immobilization conditions in PE multilayer systems may affect the redox site structure of Cyt-c and the thermodynamics, mechanism, and kinetics of the ET reactions.

Experimental Section

Materials. The sodium salts of PSS (MW: ∼70 kDa), polyallylamine hydrochloride (PAH, MW: ∼70 kDa), and poly(ethylene imine) (PEI: MW ∼50 kDa) were purchased from Aldrich. All chemicals were used as received except for PSS, which was dialyzed before use (MW: 50 kDa cut off). Horse heart Cyt-c was purchased from Sigma and purified by HPLC.

Multilayer Preparation. PEs were adsorbed by dipping the electrode, for 30 min, into a solution containing either positively or negatively charged polyelectrolytes.[8] The PE concentration in the solution was 1 mM. Except for PEI, these solutions also included 0.5 M NaCl. For all coatings, the PEI was adsorbed to the electrode to create an excess positive charge on the surface, which then allowed adsorption of the polyanion PSS. Further layers were created by alternating polycation (PAH, PEI) or polyanion (PSS) adsorption.

Protein Adsorption. For protein binding, the PE-coated electrodes were inserted into the electrochemical cell containing 0.3 μM Cyt-c, 12.5 mM potassium phosphate buffer (pH 7), and 12.5 mM K_2SO_4. During the adsorption process, the potential was set to −0.5 V (vs Ag/AgCl). Progress of adsorption was controlled by monitoring the SERR signal, which was found to increase steadily until it reached a constant level after ca. 10−15 min.

SERR Experiments. SERR spectra were measured at ambient temperature with the 413 nm excitation line of a Kr^+ laser (Coherent Innova 300) using a LabRAM spectrograph (HR800) equipped with a liquid-nitrogen-cooled CCD camera. The spectral resolution was 2 cm^{-1}, and the wavenumber increment per pixel was 0.57 cm^{-1}. The laser beam (5 mW) was focused onto the rotating Ag electrode that was mounted in a home-built electrochemical cell, which includes a Pt wire and an Ag/AgCl electrode as a counter and reference electrode, respectively. All potentials cited in this work refer to the Ag/AgCl electrode. In time-resolved experiments the potential jumps at the electrode were synchronized with the SERR detection using a home-built pulse delay generator that triggered the potentiostat and an optoelectronic laser intensity modulator. Details of the electrochemical setup and the potential-jump SERR method are given elsewhere.[18]

After background subtraction, the SERR spectra were subjected to a component analysis.[29] In this approach, the complete spectra of individual components are fitted to the experimental spectra with their relative amplitudes being the only adjustable parameters.

Quartz Crystal Microbalance Measurements. Quartz crystal microbalance (QCM) measurements were carried out using a Q-Sense D300 device equipped with a flow cell (Q-Sense AB, Vastra Frolundra, Sweden). A gold-coated 5 MHz AT-cut quartz crystal was excited at its third overtone (∼15 MHz) and the change in the resonance frequency (ΔF) was recorded. The Sauerbrey equation was used to calculate the mass of the adsorbed layers from ΔF values.[30] After the QCM electrodes were cleaned with piranha solution, a PEI layer was deposited, followed by a thorough rinse with water. Layers of PSS/Cyt-c or PSS/PAH/PSS/Cyt-c were then adsorbed onto the QCM electrodes. Changes in frequency were recorded for each adsorption step.

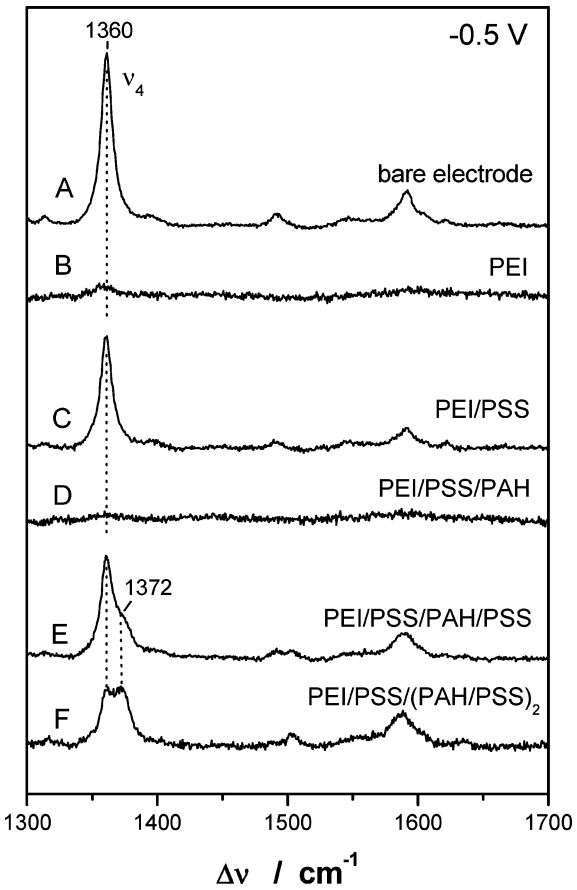

Figure 1. SERR spectra of Cyt-c immobilized on Ag electrodes with and without PE coatings. Spectra were measured with 413 nm excitation at an electrode potential of −0.5 V. The intensity scale of spectrum F is expanded by a factor of 3 for a better comparison.

Results

Adsorption of Cyt-c on PE-Coated Electrodes. Cyt-c exhibits a positively charged domain around the exposed heme edge that allows electrostatic binding to anionic surfaces.[19,20,31] This mode of binding also dominates in the case of PE-coated electrodes. An intense SERR spectrum of Cyt-c is observed for an Ag electrode that is coated first with cationic PEI and subsequently with anionic PSS (Figure 1C). The spectrum is very similar to the one measured from a "bare" electrode at −0.5 V (Figure 1A) that was covered by specifically adsorbed chloride anions. Both spectra displayed the characteristic signature of reduced Cyt-c[32], as indicated, for instance, by the prominent band at 1360 cm^{-1} (ν_4), whereas, as expected, no contribution from the oxidized Cyt-c was detectable. Conversely, no SERR spectrum was obtained when the electrode was solely covered by PEI (Figure 1B) or PE multilayers terminated by positively charged PAH (Figure 1D).

This pattern was preserved upon increasing the number of PE layers, and SERR spectra were only obtained with multilayers terminated by PSS. However, with the increasing number of PE layers, we note a growing-in of a band at 1372 cm^{-1} that is indicative for the oxidized Cyt-c (ν_4).[33] The SERR intensity

was monitored as a function of time after the addition of Cyt-c to the electrochemical cell. It was found that at electrodes coated with PSS-terminated layers, maximum SERR intensity is reached after 10−15 min, whereas for bare electrodes, the maximum SERR intensity was measured quasi instantaneously. Furthermore, the maximum SERR intensity decreases only slightly from Cyt-c at the bare electrode to Cyt-c at a PEI/PSS-coated electrode, as is documented by the spectra shown in Figure 1A,C that are plotted on the same scale. Only a slightly lower intensity is observed for the 1360 cm^{-1} band on the PEI/PSS/PAH/PSS-coated electrode as compared to the PEI/PSS coating (Figure 1C,E). However, the spectrum in Figure 1E displays a distinct shoulder at 1372 cm^{-1}, originating from oxidized Cyt-c species for which the RR cross sections are lower, by a factor of ca. 3, than those for the reduced species.[34] Thus, if all the Cyt-c molecules that contribute to the SERR spectrum were in the reduced state, the intensity of the 1360 cm^{-1} band would be at least as high as that observed for the PEI/PSS coating (Figure 1C). These findings imply that for the PEI/PSS/PAH/PSS coating, either the amount of immobilized Cyt-c is larger or the surface enhancement is at least as strong as for the PEI/PSS coating.

We have, therefore, employed QCM to determine the amount of adsorbed Cyt-c. For PEI/PSS/Cyt-c and PEI/PSS/PAH/PSS/Cyt-c, the surface concentration of Cyt-c was found to be 10 and 11 pmol/cm^2, respectively. This finding implies that, within the experimental accuracy, the amount of immobilized protein is the same for both coatings. This quantity would correspond to a monolayer coverage on the PE coating as judged from geometrical considerations.

Furthermore, the QCM data indicate that the surface enhancement of the immobilized Cyt-c must be largely the same for both the PEI/PSS and the PEI/PSS/PAH/PSS coatings. This conclusion is likely to be true also for the PEI/PSS/$(PAH/PSS)_2$-coated electrode, for which the SERR spectrum is shown on a three-times expanded scale (Figure 1F). In this spectrum, the ν_4 bands of the reduced and oxidized species display equal relative intensities which, taking into account the lower RR cross section for the ferric heme, would correspond to a peak height similar to that in the PEI/PSS system if all Cyt-c molecules were in the reduced state.

Structural Changes of Cyt-c on PE Layers. A careful inspection of the SERR spectra reveals that the bound Cyt-c exists in different states, which can be determined quantitatively by means of the component analysis.[29] In this approach, the experimental spectra are simulated by a superposition of the spectra of the individual species (components) involved. These component spectra have been determined previously for the various conformational states of Cyt-c that are formed upon binding to anionic or hydrophobic surfaces, at different pH in aqueous solution, or in the presence of denaturants.[33] It was found that, in addition to the reduced and oxidized forms of the native Cyt-c denoted as state B1, oxidized species of state B2 are formed upon immobilization of Cyt-c to the PE-coated electrodes. In state B2, the Met-80 ligand is displaced from the heme iron and the coordination site either remains vacant or is occupied by a His residue to form a five-coordinated high-spin (5cHS) and six-coordinated low-spin (6cLS) state, respectively.[4,33] The change in the ligation pattern can be monitored by the marker bands between 1450 and 1650 cm^{-1}, which display a ca. 10 cm^{-1} downshift upon transition from the 6cLS to the 5cHS state. The replacement of the Met axial ligand (B1) by a His (B2), which leaves the spin configuration and coordination number unchanged, is reflected by smaller frequency shifts but by a dramatic intensity decrease of the ν_{10} at ca. 1635 cm^{-1}. Thus, the individual component spectra reveal sufficiently large differences to allow a reliable quantification of their individual contributions to the experimental SERR spectra.[29] This has been demonstrated previously for Cyt-c adsorbed on bare Ag electrodes where the same species are formed.[4] In that study, it was shown that the changes of the coordination sphere of the heme are associated with a significant negative shift of the redox potential from +0.06 V of B1 to −0.39 (B2, 6cLS) and −0.34 V (B2, 5cHS).[4]

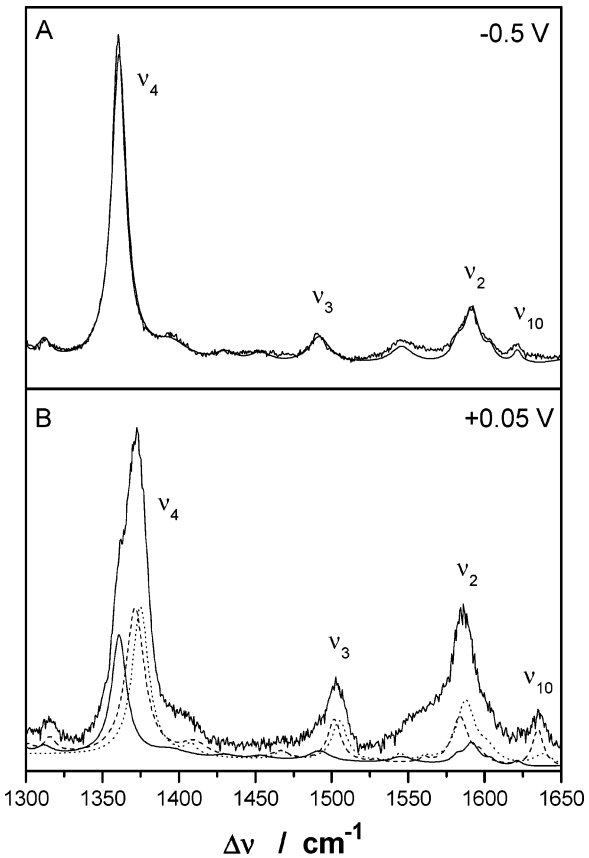

Figure 2. SERR spectra of Cyt-c adsorbed on a PEI/PSS-coated electrode at different potentials: (**A**) −0.5 V, and (**B**) +0.05 V. The solid, dashed, and dotted lines belong to the component spectra of $B1^{red}$, $B1^{ox}$, and $B2^{ox}$ respectively.

The component analysis of the SERR spectra is illustrated for Cyt-c on the PEI/PSS-coated electrode (Figure 2). At +0.05 V, the spectrum includes contributions from all three oxidized forms, B1 and the 6cLS and 5cHS species of state B2, whereas at −0.5 V, only the reduced form of B1 is found. All measured spectra showed two additional bands at 1565 and 1600 cm^{-1}, which do not originate from any of the Cyt-c species and that have been subtracted from the spectra displayed in Figure 2.

In analogy to previous findings for bare and SAM-coated electrodes,[4,20,35] the interfacial processes of the immobilized Cyt-c can be described by a square reaction scheme (Figure 3), in which, for the sake of simplicity, the 5cHS and 6cLS forms of B2 are summarized as "B2". This approximation is justified since both substates constitute a rapid coordination equilibrium. Under stationary conditions, the reduced forms of B2 are not formed to a detectable extent at any potential of PE-coated electrodes. In this respect, the behavior of the immobilized Cyt-c is similar to that of electrodes coated with carboxyl-terminated SAMs where the reduced B2 species were found to be readily converted to the reduced B1 state.[18,35] However, the reduced B2 is observed as an intermediate in potential jump experiments

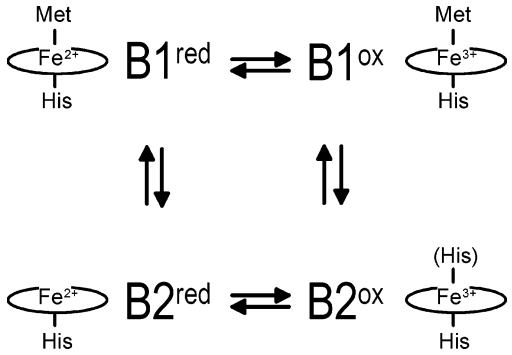

Figure 3. Reaction scheme for the redox and conformational transitions of Cyt-c adsorbed on PE-coated electrodes.

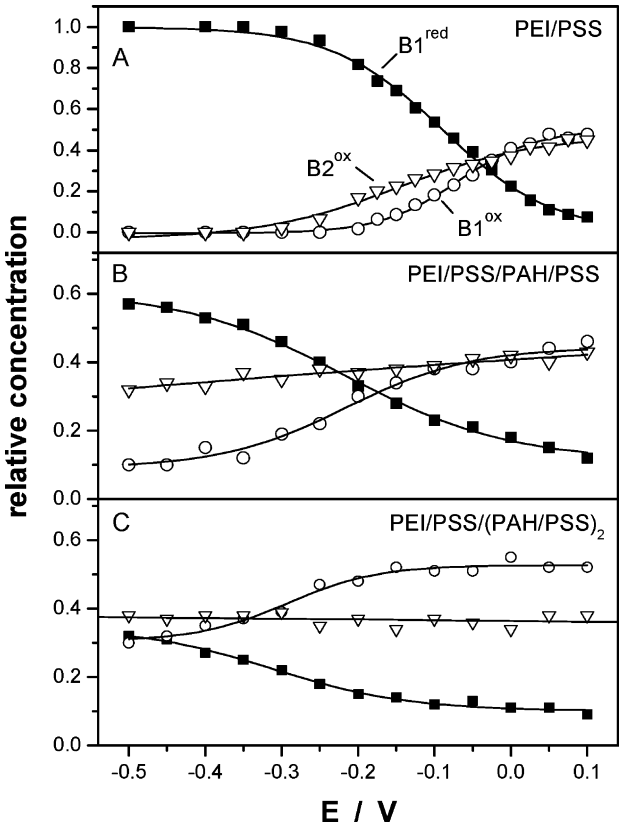

Figure 4. Relative concentrations of $B1^{red}$ (solid squares), $B1^{ox}$ (open circles), and $B2^{ox}$ (open triangles) determined as a function of the electrode potential for different PE coatings: (**A**) PEI/PSS, (**B**) PEI/PSS/PAH/PSS, and (**C**) PEI/PSS/$(PAH/PSS)_2$.

(vide infra). The amplitudes of the component spectra that are obtained from the component analysis are then converted into relative concentrations using the proportionality factors determined previously.[34]

Potential-Dependent Redox and Conformational Equilibria. Relative concentrations of the various Cyt-c species were determined from the SERR spectra measured in a potential range from −0.5 to +0.1 V. Prior to the spectroscopic measurement, the protein was kept at each potential for ca. 1 min, which was found to be sufficient to achieve redox equilibrium conditions. For a PEI/PSS-coated electrode, the potential dependence of the relative concentrations is shown in Figure 4A.

At −0.5 V, Cyt-c is completely in the reduced form of the native B1 state, $B1^{red}$. Upon increasing the potential, the portion of the oxidized states increases at the expense of $B1^{red}$. The oxidized Cyt-c includes contributions from $B1^{ox}$ and $B2^{ox}$. At +0.1 V, the contribution of the $B2^{ox}$ state is ca. 41(±5)% of the total immobilized Cyt-c (Table 1). The apparent redox potential E_0 of the B1 species was determined from a Nernstian plot, yielding a value of $E_0 = -0.03 \pm 0.01$ V. However, the redox process occurs over a wide potential range, as reflected by the low apparent number of transferred electrons, $n = 0.48 \pm 0.05$ determined from the Nernstian analysis (Table 1).

TABLE 1: Cytochrome *c* Binding and Redox Properties on Electrodes Coated with Polyelectrolyte Multilayers

	PEI/PSS	PEI/PSS/ PAH/PSS	PEI/PSS/ $(PAH/PSS)_2$
Cyt-c surface coverage[a]	10 pmol/cm^2	11 pmol/cm^2	
exp. redox potential of B1[b]	−0.03 V	−0.21 V	−0.32 V
redox potential shift[c]	−0.09 V	−0.27 V	−0.38 V
corr. redox potential shift[d]	−0.04 V	−0.19 V	−0.26 V
n[b]	0.48	0.24	0.42
% $B2^{ox}$ at +0.1 V	41	43	40
% redox activity[e]	100	49	20

[a] Determined by QCM measurements. [b] Determined from the Nernst analysis of the SERR spectroscopic data. [c] Difference with respect to the redox potential of Cyt-c in solution at pH 7.0 (+0.06 V).[16] [d] Corrected for the interfacial potential drop estimated according to ref 18. [e] Portion of immobilized Cyt-c that participates in the redox process.

The relative concentrations of the various Cyt-c species, as a function of the applied potential, change drastically upon increasing the number of PE layers (Figure 4B,C). The redox potential of the native state B1 displays large downshifts to -0.21 ± 0.01 and -0.32 ± 0.02 V for the PEI/PSS/PAH/PSS- and PEI/PSS/$(PAH/PSS)_2$-coated electrode, respectively. The limiting concentration of $B2^{ox}$ remains largely constant with ca. 40%. The n values were determined to be 0.24 ± 0.02 and 0.42 ± 0.07 for the PEI/PSS/PAH/PSS- and PEI/PSS/$(PAH/PSS)_2$-coated electrode, respectively.

Whereas for the PEI/PSS coatings, all Cyt-c molecules participate in the redox process, the portion of proteins that is electroactive within the potential range under investigation is reduced to 49% and 20% with increasing number of PE layers for the PEI/PSS/PAH/PSS- and PEI/PSS/$(PAH/PSS)_2$-coated electrode, respectively.

Dynamics of Electron Transfer and Conformational Transitions. The dynamics of the immobilized Cyt-c was studied for PEI/PSS- and PEI/PSS/PAH/PSS-coated electrodes. For PEI/PSS coatings, time-resolved SERR experiments were carried out employing potential jumps from −0.5 to +0.1 or −0.04 V to probe the oxidation of the immobilized $B1^{red}$. An example is given in Figure 5A, which shows the time dependence of the relative concentrations as a function of delay time following a potential jump from −0.5 to +0.1 V.

$B1^{red}$ decreases with the delay time relative to the potential jump, whereas the concentration of $B1^{ox}$ is increased. The SERR spectra also include a small portion (up to 10%) of $B2^{ox}$, which might be formed within the first 100 ms, and then remains constant up to 800 ms. However, it cannot be ruled out that fresh sample conditions are not completely fulfilled in the time-resolved experiments and a small portion of $B2^{ox}$ is accumulated during the repetitive potential jumps.

Thus we have restricted the kinetic analysis on the time scale between 0 and 800 ms to the ET reactions between $B1^{red}$ and $B1^{ox}$. The mean values of the rate constants for the oxidation of $B1^{red}$ were found to be 1.2 ± 0.4 s^{-1} and 0.08 ± 0.04 s^{-1} for an overpotential (η) of −0.13 and +0.01 V, respectively. The corresponding rate constants for the reduction of $B1^{ox}$ were determined to be 0.11 ± 0.03 s^{-1} and 0.14 ± 0.07 s^{-1} from the equilibrium constant defined by the Nernst equation.

In the same way, we have analyzed the potential jump experiments for Cyt-c immobilized on PEI/PSS/PAH/PSS

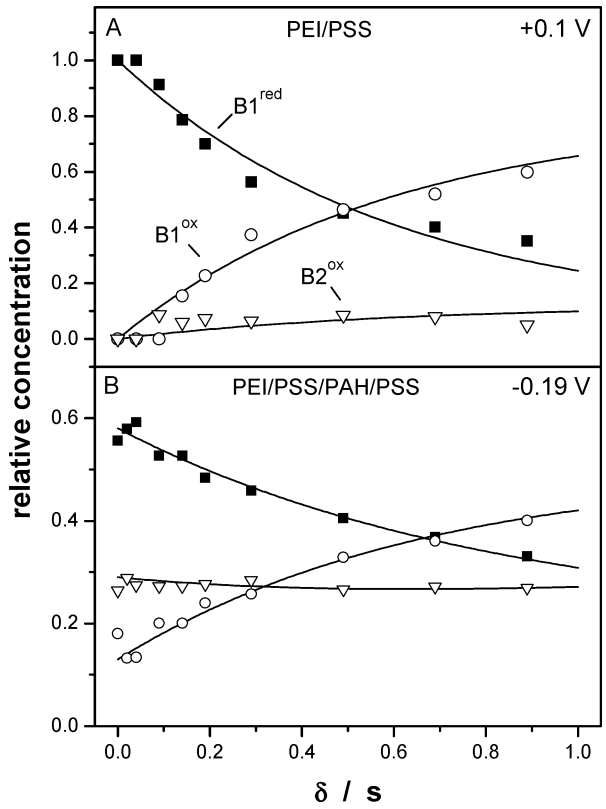

Figure 5. Relative concentrations of $B1^{red}$ (solid squares), $B1^{ox}$ (open circles), and $B2^{ox}$ (open triangles), determined as a function of delay time after a potential jump, for different overpotentials η: (**A**) PEI/PSS-coated electrode ($\eta = -0.13$ V), and (**B**) PEI/PSS/PAH/PSS-coated electrode ($\eta = -0.02$ V). The solid lines represent a fit to the experimental data according to the kinetic model described in the text.

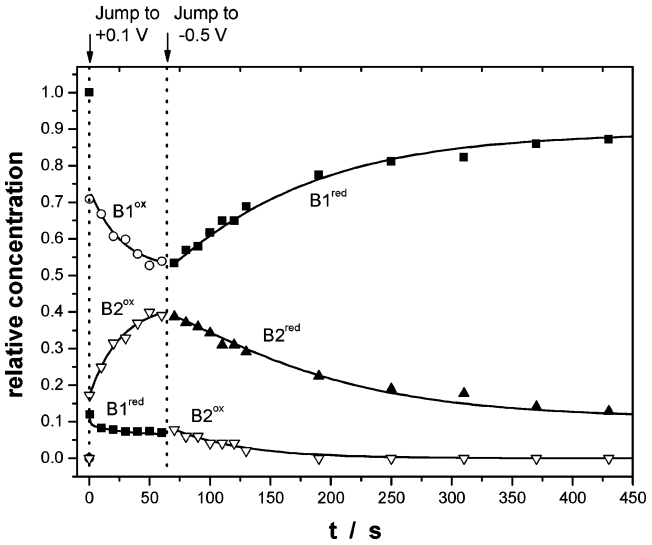

Figure 6. Time dependence of the relative concentrations of $B1^{red}$ (solid squares), $B1^{ox}$ (open circles), $B2^{ox}$ (open triangles), and $B2^{red}$ (solid triangles) adsorbed on a PEI/PSS-coated electrode after a potential jump from -0.5 V to $+0.1$ V ($t = 0$ s) and back to -0.5 V at 65 s, indicated by the vertical line. The solid lines represent a fit to the experimental data according to the kinetic model described in the text.

coatings for potential jumps that correspond to overpotentials of -0.02 , -0.16 , and -0.31 V, respectively. An example is given in Figure 5B for a potential jump from -0.5 to -0.19 V, corresponding to an overpotential of -0.02 V. $B2^{ox}$ is already present at the initial potential of -0.5 V and does not change with time. Within the experimental accuracy, the heterogeneous ET rate constant for the transition $B1^{red} \rightarrow B1^{ox}$ of 0.87 ± 0.4 s^{-1} was found to be independent of the overpotential. Furthermore, the value is more than 10 times higher than the rate constant determined for the PEI/PSS coating at an overpotential of ca. 0 V.

At ca. 800 ms, the three species $B1^{red}$, $B1^{ox}$, and $B2^{ox}$ have not reached thermodynamic equilibrium since their relative concentrations differ substantially from those determined in stationary SERR experiments (cf. Figure 4A). The slower interfacial processes were probed for PEI/PSS-coated electrodes by measuring the SERR spectra after intervals of 10 s, following a potential jump from -0.5 to $+0.1$ V (Figure 6).

Within the first time interval the contribution of $B1^{red}$ further drops to ca. 12% while $B1^{ox}$ and $B2^{ox}$ increase to ca. 71% and 17%, respectively. Subsequently, both $B1^{red}$ and $B1^{ox}$ slowly decay to their equilibrium values while $B2^{ox}$ increases to its equilibrium value of 40%.

On the basis of the Scheme 1,

SCHEME 1

$$B1^{red} \rightleftarrows B1^{ox} \rightleftarrows B2^{ox}$$

which is derived from Figure 3, a good fit to the experimental data could be achieved with a rate constant of 0.03 ± 0.01 for the conformational transition $B1^{ox} \rightarrow B2^{ox}$, and 0.04 ± 0.02 s^{-1} for the back reaction $B2^{ox} \rightarrow B1^{ox}$. On the second time scale, the oxidation of $B1^{red}$ proceeds with a rate constant of 0.05 ± 0.01 s^{-1}, whereas the rate constant of the reverse reaction is ca. 10 times smaller.

When, after 60 s, the potential is reset to -0.5 V, within 10 s, ca. 53% of the immobilized Cyt-c molecules are converted to $B1^{red}$ and no $B1^{ox}$ can be detected. The major portion of state B2 (>90%) was found to have been reduced to $B2^{red}$ within this time interval, implying that the ET rate constant for the reduction of $B2^{ox}$ is larger than 0.25 s^{-1}. The subsequent processes mainly include the conformational transition between $B2^{red}$ and $B1^{red}$, but, in addition, we note a further slow decay of $B2^{ox}$. Although conversion of $B2^{ox}$ to $B1^{ox}$ and subsequent reduction to $B1^{red}$ (Scheme 1) cannot be safely ruled out, it appears to be more likely that the decay of $B2^{ox}$ occurs via the alternative route according to Scheme 2.

SCHEME 2

$$B2^{ox} \rightleftarrows B2^{red} \rightleftarrows B1^{red}$$

On the basis of this reaction scheme, one obtains a rate constant for the slow ET of the residual (9%) of $B2^{ox}$ to $B2^{red}$ of ca. 0.02 ± 0.01 s^{-1}, whereas conformational transition of $B2^{red}$ to $B1^{red}$ takes place with a rate constant of 0.009 ± 0.001 s^{-1} (Table 2).

Time-resolved measurements at longer time scales were also carried out for a jump from $+0.1$ to -0.4 V. Also in this case, the "fast" ET from $B2^{ox}$ could not be resolved but the slow phase was found to be similar to that for the potential jump to -0.5 V. The conformational transition $B2^{red} \rightarrow B1^{red}$ was determined to be 0.02 ± 0.01 s^{-1}. The rate constants derived from the time-resolved SERR experiments are summarized in Table 2.

Discussion

Immobilization of Cyt-c in PE Multilayers. The SERR intensity of Cyt-c on PEI/PSS coatings is ca. 1.5−2 times weaker than on the "bare" electrode (Figure 1A,C). Previous

TABLE 2: Rate Constants for the Heterogeneous Electron Transfer and Conformational Transitions of Cytochrome *c* Immobilized on Electrodes Coated with PE Multilayers

PE system	reaction	E_f/V[a]	η/V[b]	k/s^{-1}[c]
		Electron Transfer		
PEI/PSS	$B1^{red} \rightarrow B1^{ox}$	−0.04	+0.01	0.08 ± 0.04
		+0.1	−0.13	1.2 ± 0.4; 0.05 ± 0.01
	$B1^{ox} \rightarrow B1^{red}$	−0.04	+0.01	0.14 ± 0.07
		+0.1	−0.13	0.11 ± 0.03; 0.004 ± 0.0002
	$B2^{ox} \rightarrow B2^{red}$	−0.5		> 0.25; 0.02 ± 0.01
PEI/PSS/PAH/PSS	$B1^{red} \rightarrow B1^{ox}$	−0.19[d]	−0.02	0.87 ± 0.4
		Conformational Transitions		
PEI/PSS	$B1^{ox} \rightarrow B2^{ox}$	+0.1		0.03 ± 0.01
	$B2^{ox} \rightarrow B1^{ox}$	+0.1		0.04 ± 0.02
	$B2^{red} \rightarrow B1^{red}$	−0.5		0.009 ± 0.001
		−0.4		0.02 ± 0.01
	$B1^{red} \rightarrow B2^{red}$	−0.5		0.001 ± 0.0001

[a] Electrode potential E_f at which the reaction was monitored. [b] Overpotential as defined by the difference between E_f and the redox potential (Table 1). [c] Rate constants determined from time-resolved SERR experiments as described in the text. [d] The same rate constants were determined for overpotentials of −0.16 and −0.31 V.

studies have shown that the surface enhancement decreases by a factor of ca. 10 when Cyt-c is separated from the electrode by ca. 25 Å.[18] Assuming a thickness of the PEI and PSS layers of ca. 10 and 13 Å, respectively,[36] a similar intensity drop is expected for comparable protein surface concentrations. The observed intensity ratio, therefore, suggests a 5 times larger coverage on the PEI/PSS-coated electrode. This conclusion is confirmed by QCM determinations that reveal an amount of Cyt-c bound to PEI/PSS equivalent to full monolayer coverage, while for "bare" Ag surfaces it was estimated to be less than 20% of the geometrically possible coverage.[37] Thus, the data are consistent with peripheral binding of Cyt-c on the PEI/PSS-coated electrode.

Addition of further PE layers (PEI/PSS/PAH/PSS and PEI/PSS/$(PAH/PSS)_2$) does not affect the SERR intensity significantly (Figure 1), whereas QCM measurements indicate approximately the same amount of bound protein as for the PEI/PSS coating. This observation implies that, unlike PEI/PSS coatings, binding of Cyt-c to PEI/PSS/PAH/PSS and PEI/PSS/$(PAH/PSS)_2$ does not occur in the PSS/solution interface but leads to a penetration into the PE multilayer. The highly positively charged Cyt-c that can be regarded as a polycation may effectively compete with PAH for binding of PSS in the more flexible multilayer systems. Thus, we conclude that PSS partially wraps around Cyt-c and thus overcompensates the positive charges on the protein surface such that the resulting PSS/Cyt-c complex migrates toward the positively charged electrode, thereby causing a rearrangement of the multilayer. This process, which can be compared with the electrophoretic migration of biopolymers, may be reflected by the slow increase of the SERR signal after immersing the PE-coated electrode into the Cyt-c solution. This interpretation is further in line with the redox potential shifts and the ET kinetics (vide infra).

Redox Potential Shifts and Conformational Equilibria of Peripherally Bound Cyt-c. Immobilization on PSS-terminated PE multilayers causes a partial transition to the conformational state B2 and a negative shift of the redox potential. *Qualitatively* the same effects have been observed for Cyt-c immobilized on carboxylate-terminated SAMs.[18,20] Within the framework of the plane-of-electron-transfer (PET) model developed by Smith and White,[38] it was shown that, for these systems, the redox potential shifts originate from the potential drop across the electrode/SAM/protein interfaces.[18]

To adopt this model to Cyt-c on PSS-terminated PE multilayers, we have to assume a net charge of zero within each layer, a constant thickness (i.e., 3 nm per PE double layer[36,39]), and the peripheral attachment of Cyt-c on the terminating PSS layer. For the PEI/PSS-coated electrode, the redox potential shift of the bound Cyt-c is then calculated to be −0.05 V. The agreement with the experimental value of −0.09 V is poorer than that for the Cyt-c on SAM-coated electrodes but still acceptable, taking into account the quite severe underlying assumptions.

Also, the electric-field dependence of the conformational equilibrium can be qualitatively understood on the basis of the PET model. The predicted decrease of the electric field strength at the Cyt-c binding site with decreasing electrode potential is in line with the complete re-conversion to the native state B1 at potentials below −0.4 V (Figure 4).[20]

Redox Potential Shifts and Conformational Equilibria of Integrated PSS/Cyt-c Complexes. For PEI/PSS/PAH/PSS and PEI/PSS/$(PAH/PSS)_2$, the PET model underestimates the redox potentials shifts by 0.19 and 0.26 V, respectively (Table 1). The strong discrepancy confirms that Cyt-c does not peripherally bind to these coatings and that the large downshifts of the redox potentials cannot arise solely from the potential drop across the multilayers.

Peripheral binding of Cyt-c to better structured systems, such as SAMs or, to a certain extent, PEI/PSS, is established via electrostatic interactions of a few cationic amino acid residues around the exposed heme edge.[40] In contrast, the enclosure of Cyt-c by PSS that is most likely associated with the integration into multilayers (vide supra) provides a high density of negative charges around the protein. Thus, the ferrous state of the heme is expected to be destabilized with respect to the ferric form, corresponding to a downshift of the redox potential. Such an effect has been theoretically predicted and experimentally observed for the tetraheme protein cytochrome c_3 adsorbed on SAMs with carboxylate headgroups.[41] Conversely, comparable shifts have not yet been found for Cyt-c immobilized on surfaces covered with anionic SAMs and specifically adsorbed anions,[4,18,20] implying that the electrostatic interactions of PSS with Cyt-c are qualitatively different.

The formation of such PSS/Cyt-c complexes is consistent with the fact that only for PEI/PSS/PAH/PSS and PEI/PSS/$(PAH/PSS)_2$ coatings the portion of B2 appears to be largely potential-independent and about the same for both PE multilayers. This interpretation is also in line with recent findings by Gong et al.[42] These authors have shown that complex formation of ferric Cyt-c with PSS in solution may lead to a species which, according to the CD and UV−vis spectra, can be identified as the 6cLS form of the conformational state B2.[33,42]

Electron Transfer and Conformational Dynamics of Peripherally Bound Cyt-c. In a previous work, we have determined a reorganization energy of 25.1 kJ/mol for Cyt-c electrostatically adsorbed on SAM-coated electrodes.[23] Based on this value, an overpotential of −0.14 V should cause a 14-fold acceleration of the ET rate with respect to zero driving force. In good agreement with this prediction, we observe that a similar change of the driving force for the PEI/PSS coating results in an increase of the fast component of the B1 oxidation rate by a factor of 15 (Table 2). Also, the formal heterogeneous ET rate constant of 0.1 s^{-1} is nearly identical to the value of 0.07 s^{-1} determined for Cyt-c at SAM coatings of comparable thickness (ca. 24 Å).[25] We conclude, therefore, that for the B1 state of Cyt-c peripherally bound to PEI/PSS coatings, the

heterogeneous ET reaction is nonadiabatic (long-range electron tunneling) and the electronic coupling as well as its distance dependence and the reorganization energy are similar to those on SAM coatings.

The same conclusions can be derived from the fast component of the reduction kinetics of the conformational state B2, which is converted to $B1^{red}$ with a rate constant larger than 0.25 s^{-1}. ET to $B2^{red}$, which is in the 5cHS configuration, most likely occurs via the 5cHS substate of $B2^{ox}$, which forms a rapid coordination equilibrium with the 6cLS form of $B2^{ox}$. Thus, reduction is controlled by the redox potential of the 5cHS form, which is −0.34 V at the "bare" electrode. Assuming the same redox potential shift as in the case of the B1 state (i.e., −0.09 V), the overpotential for this ET process is ca. −0.07 V. Then the lower limit estimated for the fast phase of the ET points to a formal heterogeneous ET rate constant that is comparable to that of B1.

The slow kinetic components of the reduction processes of $B1^{ox}$ and $B2^{ox}$, which both exhibit small amplitudes, are attributed to the coupling of the ET with slower non-Faradaic processes. Probably, a small fraction of the adsorbed Cyt-c requires a rate-limiting reorientation to achieve a configuration that is favorable for ET. An analogous explanation may hold for the conformational transition $B2^{red} \rightarrow B1^{red}$, which is found to be much slower than the conformational transitions in the oxidized state.

Electron Transfer and Conformational Dynamics of Integrated PSS/Cyt-c Complexes. The rate of reduction of $B1^{ox}$ on PEI/PSS/PAH/PSS was found to be independent of the overpotential and similar to the value determined for the PEI/PSS system at an overpotential of −0.13 V. This peculiar behavior points to a more complex ET mechanism that arises from the penetration of the protein into the PAH/PSS double layer. The specific PSS/Cyt-c interactions in these systems cause a large negative shift of the redox potential and are likely to have also a pronounced effect on the reorganization energy. Moreover, the individual PSS/Cyt-c complexes that are integrated into the PE multilayers will differ with respect to the distance and orientation relative to the electrode as well as in terms of the specific electrostatic interactions with the charged sulfonate headgroups of PSS. This heterogeneity is likely to cause a distribution of electronic couplings, redox potentials, and reorganization energies, corresponding to a wide distribution of rate constants. For such a system, the electronic communication with the electrode is expected to be largely restricted to the subpopulation of proteins that provides the fastest electron tunneling due, for instance, to a particularly favorable orientation and close proximity to the electrode surface. For the remaining species, reduction and oxidation most likely proceed via protein-to-protein ET. In fact, Beissenhirtz et al.[28] have recently shown that interprotein ET of Cyt-c incorporated into PE multilayers occurs with a rate constant of ca. 1.5 s^{-1}, which is similar to the value determined in the present study for the PEI/PSS/PAH/PSS coatings. This finding, as well as the overpotential independence of the oxidation/reduction rate, suggests that interprotein ET is the rate-limiting step of the overall redox process at PAH/PSS-containing coatings.

Consistent with the view of kinetically different PSS/Cyt-c complexes, the low redox activity on PEI/PSS/PAH/PSS and PEI/PSS/$(PAH/PSS)_2$ coatings (Table 1; Figure 4B,C) can be attributed to species with very slow ET kinetics.

Conclusions

1. Cyt-c adsorbs electrostatically to the surface of PEI/PSS coatings and penetrates into PE coatings involving additional PAH/PSS double layers.

2. The redox activity of Cyt-c on PEI/PSS coatings is fully preserved, but the apparent redox potential is negatively shifted, due to the interfacial potential drop. The formal ET rate constant (0.1 s^{-1}) is consistent with a long-range electron tunneling through an ordered PE layer. The redox process is coupled with a reversible transition between the native form B1 and the conformational state B2.

3. For Cyt-c integrated into PEI/PSS/$(PAH/PSS)_n$ coatings, the fraction of B2 is electrochemically inactive within the range from +0.1 to −0.5 V. The overall redox activity is reduced to 49% ($n = 1$) and 20% ($n = 2$). The rate of reduction is limited by inter-protein ET.

4. Developing bioelectronic devices on the basis of redox proteins in PSS-containing PE-multilayers does not appear to be a promising approach in view of the slow heterogeneous ET, the broad redox transitions, and partly low redox activity as well as the coupling with protein conformational transitions found for Cyt-c.

Acknowledgment. This work was supported by the Deutsche Forschungsgemeinschaft (SfB 448, C1).

References and Notes

(1) Willner, I.; Katz, E. *Angew. Chem., Int. Ed*. **2000**, *39*, 1180−1218.
(2) Holt, R. E.; Cotton, T. M. *J. Am. Chem. Soc*. **1989**, *111*, 2815−2821.
(3) Yang, M. S.; Chung, F. L.; Thompson, M. *Anal. Chem*. **1993**, *65*, 3713−3716.
(4) Wackerbarth, H.; Hildebrandt, P. *Chem. Phys. Chem*. **2003**, *4*, 714−724.
(5) Armstrong, F. A.; Hill, H. A. O.; Walton, N. J. *Acc.Chem. Res*. **1988**, *21*, 407−413.
(6) Ulman, A. *Introduction to Ultrathin Organic Films. From Langmuir-Blodgett to Self-Assembly*; Academic Press: Boston, 1991; p 279.
(7) He, J. A.; Samuelson, L.; Li, L.; Kumar, J.; Tripathy, S. K. *Adv. Mater*. **1999**, *11*, 435.
(8) Decher, G. *Science* **1997**, *277*, 1232−1237.
(9) Salloum, D. S.; Schlenoff, J. B. *Biomacromolecules* **2004**, *5*, 1089−1096.
(10) Schwinte, P.; Voegel, J. C.; Picart, C.; Haikel, Y.; Schaaf, P.; Szalontai, B. *J. Phys. Chem. B* **2001**, *105*, 11906−11916.
(11) Wittemann, A.; Ballauff, M. *Anal. Chem*. **2004**, *76*, 2813−2819.
(12) Ladam, G.; Gergely, C.; Senger, B.; Decher, G.; Voegel, J. C.; Schaaf, P.; Cuisinier, F. J. G. *Biomacromolecules* **2000**, *1*, 674−687.
(13) Caruso, F.; Möhwald, H. *J. Am. Chem. Soc*. **1999**, *121*, 6039−6046.
(14) Lvov, Y.; Ariga, K.; Ichinose, I.; Kunitake, T. *J. Am. Chem. Soc*. **1995**, *117*, 6117−6123.
(15) Lojou, T.; Bianco, P. *Langmuir* **2004**, *20*, 748−755.
(16) *Cytochrome c-A Multidisciplinary Approach*; Scott, R. A., Mauk, A. G., Eds; University Science Books: Sausalito, 1995.
(17) Fedurco, M. *Coord. Chem. Rev*. **2000**, *209*, 263−331.
(18) Murgida, D. H.; Hildebrandt, P. *J. Phys. Chem. B* **2001**, *105*, 1578−1586.
(19) Hildebrandt, P.; Stockburger, M. *Biochemistry* **1989**, *28*, 6710−6721.
(20) Murgida, D. H.; Hildebrandt, P. *Acc. Chem. Res*. **2004**, *37*, 854−861.
(21) Cotton, T. M.; Schultz, S. G.; van Duyne, R. P. *J. Am. Chem. Soc*. **1980**, *102*, 7960−7962.
(22) Dick, L. A.; Haes, A. J.; van Duyne, R. P. *J. Phys. Chem. B* **2000**, *104*, 11752−11762.
(23) Murgida, D. H.; Hildebrandt, P. *J. Phys. Chem. B* **2002**, *106*, 12814−12819.
(24) Lecomte, S.; Wackerbarth, H.; Soulimane, T.; Buse, G.; Hildebrandt, P. *J. Am. Chem. Soc*. **1998**, *120*, 7381−7382.
(25) Murgida, D. H.; Hildebrandt, P. *J. Am. Chem. Soc*. **2001**, *123*, 4062−4068.
(26) Wackerbarth, H.; Klar, U.; Günther, W.; Hildebrandt, P. *Appl. Spectrosc*. **1999**, *53*, 283−291.

(27) Lvov, Y. M.; Lu, Z. Q.; Schenkman, J. B.; Zu, X. L.; Rusling, J. F. *J. Am. Chem. Soc.* **1998**, *120*, 4073−4080.

(28) Beissenhirtz, M. K.; Scheller, F. W.; Stöcklein, W. F. M.; Kurth, D. G.; Möhwald, H.; Lisdat, F. *Angew. Chem., Int. Ed.* **2004**, *43*, 4357−4360.

(29) Döpner, S.; Hildebrandt, P.; Mauk, A. G.; Lenk, H.; Stempfle, W. *Spectrochim. Acta* **1996**, *A 51*, 573−584.

(30) Sauerbrey, G. *Z. Physik* **1959**, *155*, 206−222.

(31) Döpner, S.; Hildebrandt, P.; Rosell, F. I.; Mauk, A. G.; von Walter, M.; Buse, G.; Soulimane, T. *Eur. J. Biochem.* **1999**, *261*, 379−391.

(32) Hu, S. Z.; Morris, I. K.; Singh, J. P.; Smith, K. M.; Spiro, T. G. *J. Am. Chem. Soc.* **1993**, *115*, 12446−12458.

(33) Oellerich, S.; Wackerbarth, H.; Hildebrandt, P. *J. Phys. Chem. B* **2002**, *106*, 6566−6580.

(34) Albrecht, T.; Li, W.; Ulstrup, J.; Haehnel, W.; Hildebrandt, P. *Chem. Phys. Chem.* **2005**, *6*, 961−970.

(35) Rivas, L.; Murgida, D. H.; Hildebrandt, P. *J. Phys. Chem. B* **2002**, *106*, 4823−4830.

(36) Dong, W. F.; Ferri, J. K.; Adalsteinsson, T.; Schoenhoff, M.; Sukhorukov, G. B.; Möhwald, H. *Chem. Mater.* **2005**, *17*, 2603−2611.

(37) Hildebrandt, P.; Stockburger, M. *J. Phys. Chem.* **1986**, *90*, 6017−6024.

(38) Smith, C. P.; White, H. S. *Anal. Chem.* **1992**, *64*, 2398−2405.

(39) Dong, W. F.; Sukhorukov, G. B.; Mohwald, H. *Phys. Chem. Chem. Phys.* **2003**, *5*, 3003−3012.

(40) Zhou, J.; Zheng, J.; Jiang, S. Y. *J. Phys. Chem. B* **2004**, *108*, 17418−17424.

(41) Rivas, L.; Soares, C. M.; Baptista, A. M.; Simaan, J.; Di Paolo, R. E.; Murgida, D. H.; Hildebrandt, P. *Biophys. J.* **2005**, *88*, 4188−4199.

(42) Gong, J.; Yao, P.; Duan, H. W.; Jiang, M.; Gu, S. H.; Chunyu, L. *Biomacromolecules* **2003**, *4*, 1293−1300.